

# The Role of the Robot Mass and Velocity in Physical Human-Robot Interaction - Part I: Non-constrained Blunt Impacts

Sami Haddadin, Alin Albu-Schäffer, and Gerd Hirzinger

**Abstract**—The desired coexistence of robotic systems and humans in the same physical domain, by sharing their workspace and actually cooperating in a physical manner, poses the very fundamental problem of ensuring safety to the user. In this paper we will show the influence of robot mass and velocity during blunt unconstrained impacts with humans. Several robots with weights ranging from 15–2500 kg are impacted at different velocities with a mechanical human head mockup. This is used to measure the so-called Head Injury Criterion, mainly a measure for brain injury. Apart from injuries indicated by this criterion and a detailed analysis of chest impacts we point out that e.g. fractures of facial bones can occur during collisions at typical robot velocities. Therefore, this injury mechanism which is more probable in robotics is evaluated in detail.

## I. MOTIVATION & INTRODUCTION

In order to realize physical Human Robot Interaction (pHRI) robots and humans have to be spatially brought together, leading to the fundamental concern of how to ensure safety to the human. As Asimov already noted very early, safety has priority if robots are close to humans [1]. Intuitively it seems clear that a robot moving at maximum speed (e.g. due to malfunction) can cause high impact injury. Regarding this issue we present new insights and surprising results.

During unexpected collisions, various injury sources as e.g. fast blunt impacts, dynamic and quasi-static clamping, or being cut by sharp tools are present. Fundamental work on human-robot impacts under certain worst-case conditions and resulting injuries was carried out in [2], [3], [4], taking a look at a robot speed up to 2 m/s.

According to ISO-10218 [5], which defines new collaborative operation requirements for industrial robots, one of the following conditions always has to be fulfilled for allowing human-robot interaction: The TCP/flange velocity needs to be  $\leq 0.25$  m/s, the maximum dynamic power  $\leq 80$  W, or the maximum static force  $\leq 150$  N. In our opinion these requirements tend to be quite restrictive, too undifferentiated and strongly limit the performance of the robot as will be supported by our results.

Further important aspects concerning safety in human-robot interaction were evaluated in [6], [7], [8]. However, attempts to investigate real-world threats via impact tests at standardized crash-test facilities and use the outcome to analyze safety issues during physical human-robot interaction were to our knowledge only carried out in [4], [9] up to now. In order to quantify the potential danger emanating

from the DLR Lightweight Robot III (LWRIII), impact tests at the Crash-Test Center of the German Automobile Club (ADAC) were conducted and evaluated. The outcome of the dummy crash-tests indicated a very low injury risk with respect to evaluated injury criteria posed by rigid impacts with the LWRIII. These results presented in [4], [9] indicate that a robot, even with arbitrary mass moving not much faster than 2 m/s is not able to become dangerous to a non-clamped human head with respect to typical severity indices. These are injury indicators used in the automobile industry which for the head usually focus on its acceleration. The most prominent measure in the literature is the Head Injury Criterion (HIC) [10], defined as

$$\text{HIC}_{36} = \max_{\Delta t} \left\{ \Delta t \left( \frac{1}{\Delta t} \int_{t_1}^{t_2} \|\ddot{\mathbf{x}}_H\|_2 dt \right)^{\left(\frac{5}{2}\right)} \right\} \leq 1000 \quad (1)$$

$$\Delta t = t_2 - t_1 \leq \Delta t_{\max} = 36 \text{ ms.}$$

$\|\ddot{\mathbf{x}}_H\|_2$  is the resulting acceleration of the human head<sup>1</sup> and has to be measured in  $g = 9.81 \text{ m/s}^2$ . Since the numerical value of a severity index as the HIC is not a direct measure of injury severity, there exist mappings from most severity indices to (probability of) injury level. The injury level itself is usually expressed in terms of the Abbreviated Injury Scale (AIS) which is an internationally established definition of injury severity, classifying it from 0 (none) to 6 (fatal). A numerical HIC value below 650 represents very low injury by means of the EuroNCAP<sup>2</sup>. For further information on HIC, AIS and other Severity Indices (not only for the head but for the chest and neck as well), please refer to [4]. In Fig. 1 simu-

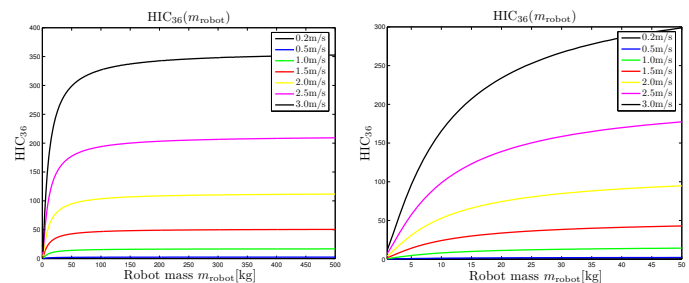


Fig. 1. Resulting Head Injury Criterion calculated from simulated 1DOF impacts between a robot with increasing mass and a dummy head model extracted from real impact data.

lated results for the HIC, resulting from a robot colliding with

<sup>1</sup> $\|\ddot{\mathbf{x}}\|_2$  =Euclidean norm

<sup>2</sup>The initial crash-tests with the LWRIII were carried out at the ADAC. They are the basis for the tests presented in this paper and are evaluated according to the EuroNCAP. This is a manufacturer independent crash-test program, based on the AIS.

S. Haddadin, A. Albu-Schäffer, and G. Hirzinger are with Institute of Robotics and Mechatronics, DLR - German Aerospace Center, Wessling, Germany samihaddadin, alin.albu-schaeffer, gerd.hirzinger@dlr.de  
This work has been partially funded by the European Commission's Sixth Framework Programme as part of the projects SMERobot<sup>TM</sup> under grant no. 011838 and PHRIENDS under grant no. 045359.

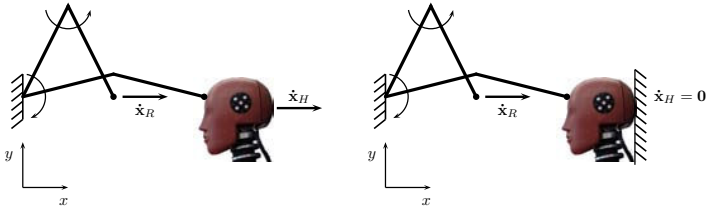


Fig. 2. Two types of blunt impacts: Without (left) and with clamping (right).

a dummy head model, which was extracted from real impact data [4], are outlined. The HIC was evaluated for robot masses up to 500 kg and graphs were obtained for impact velocities of  $\|\dot{\mathbf{x}}_R\| \in \{0.2, 0.5, 1.0, 1.5, 2.0, 2.5, 3.0\}$  m/s. They show that the HIC saturates for increasing robot mass at each impact velocity. This on the other hand indicates that at some point increasing robot mass does not result in higher HIC anymore. Consequently, no robot whatever mass it has could become dangerous at 2 m/s by means of *impact* related criteria used in the automobile industry, as long as clamping can be excluded.

Generally, there are two major types of blunt impacts: impacts with and without clamping, see Fig. 2. In this paper we will present non-constrained impact tests, verifying the above mentioned theoretical extrapolation and at the same time show that impact force is a possible and more appropriate severity index, since it indicates fractures of facial and cranial bones which can occur at typical robot speeds. In the second part of this work [11], the rarely analyzed injury in case of clamping which was motivated in [12] will be discussed. This paper is organized as follows. In Sec. II the general setup including the evaluated robots is described. Sec. III presents the results and evaluation of the impact tests and simulations for the head, followed by the analysis of the chest in Sec. IV. Finally in Sec. V a conclusion and outlook will be given.

### A. Introductory example

In order to show that the HIC is mainly depending on the impact velocity, an impact simulation with a trajectory similar to a jab was carried out with the LWRIII. This example raised out of the question where a typical punch trajectory could have its worst-case configuration concerning HIC. Therefore, a punch against a human head model at maximum joint speed of  $120^\circ/\text{s}$  was carried out and the resulting HIC was calculated. The desired trajectory was a rest-to-rest motion which start and end configuration was given by

$$\begin{aligned} \mathbf{q}_{\text{start}} &= (0 \quad -90 \quad 90 \quad -180 \quad 0 \quad 0 \quad 90)^\circ \\ \mathbf{q}_{\text{stop}} &= (0 \quad 0 \quad 90 \quad 0 \quad 0 \quad 0 \quad 0)^\circ. \end{aligned}$$

In Fig. 3 the evaluated HIC, the external force, the TCP-velocity and the reflected inertia in  $x$ -direction are given as functions of impact position. Clearly one can see the major influence of the impact velocity on HIC and the minor contribution of the reflected Cartesian inertia. Furthermore, the HIC is very low during such “punching”. This also

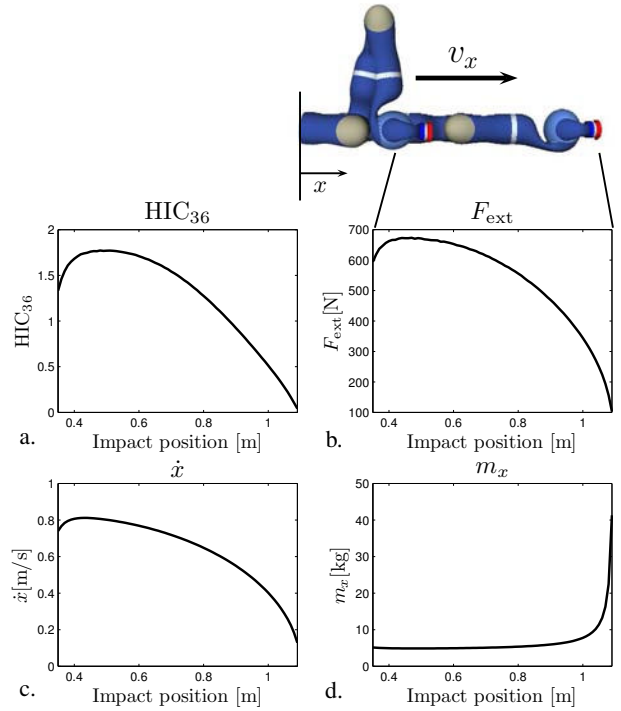


Fig. 3. Punching with the LWRIII.

motivated the choice of the robot configurations in Sec. III-A providing high Cartesian velocities for the HIC evaluation.

## II. TEST SETUP

### A. The Dummy Head

In [4] results and implications from impact tests at certified crash-test facilities of the German Automobile Club ADAC with the LWRIII were presented, see Fig. 6a. Because such crash-tests are very expensive, we decided to use the resulting outcome of these impact tests to build up a simplified setup that mimics a Hybrid III (HIII) dummy head and use it for the evaluation of other robots. In Fig. 4 (upper) this test-bed, consisting of a dummy head-neck complex, equipped with a triaxial acceleration sensor, is shown.

In Fig. 4 (lower) the HIC values obtained by the impact tests at the ADAC, i.e. with a real HIII and the ones we measured with the simplified dummy-dummy are compared. It shows that our setup is capable of reproducing very similar numerical values and therefore serves from now on as a basis for comparing different robots with respect to the Head Injury Criterion.

### B. The Impactor

Equal contact characteristics for the robots are ensured by an aluminum impactor which was mounted on the flange and was equipped with a stiff high-bandwidth force sensor, see Fig. 5. Thus, a reference body with a weight of  $\approx 1$  kg is given for all robots.

### C. Evaluated Robots

In order to cover a wide range of robots and be able to verify the saturation effect explained in [4], the LWRIII

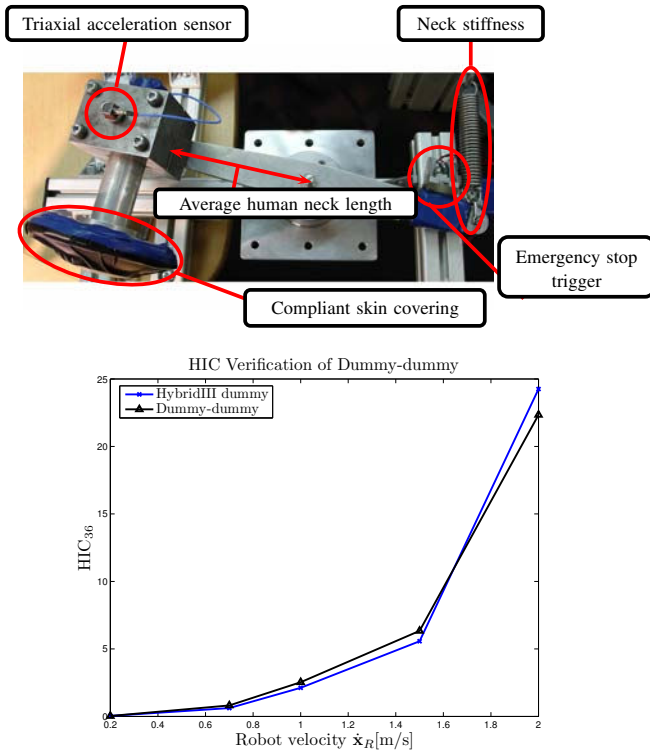


Fig. 4. Dummy-dummy adjusted to the HIII (upper). Verification of the dummy-dummy by comparing resulting HIC values obtained by real HIII crash-tests with the LWRIII (lower).

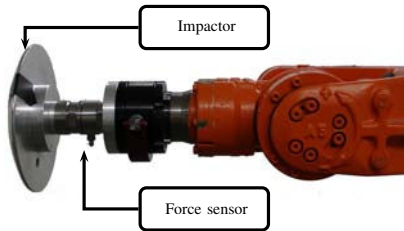


Fig. 5. Aluminum impactor mounted on the TCP flange of the manipulator.

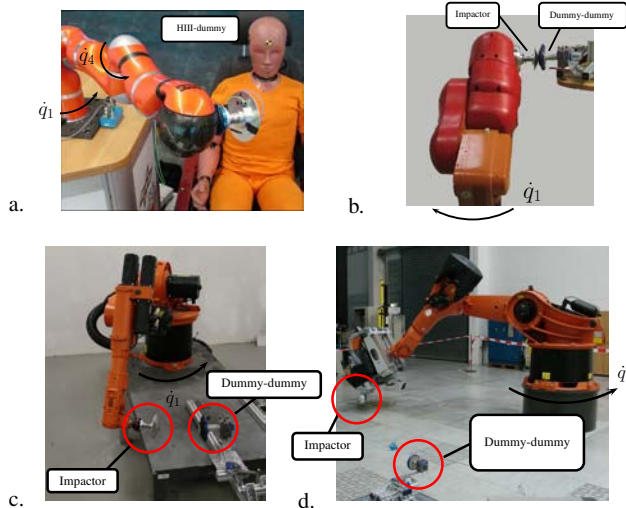


Fig. 6. Setup of impact tests with the LWRIII (a), KUKA KR3-SI (b), KUKA KR6 (c) and KUKA KR500 (d).

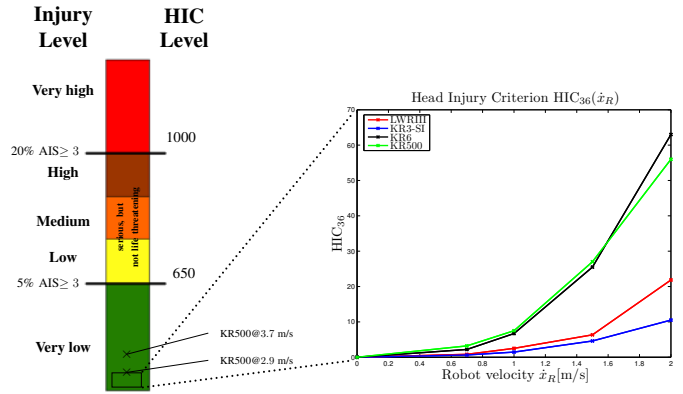


Fig. 7. Resulting HIC<sub>36</sub> values for all evaluated robots at varying impact velocities, rated according to the EuroNCAP Assessment Protocol And Biomechanical Limits.

is compared with three industrial robots<sup>3</sup>. Fig. 6 shows the setup for each of them. All industrial robots were rotating about the first axis and evaluated for the same Cartesian velocity at the Tool Center Point (TCP) as the LWRIII in [4]. The impact configurations for the robots were

$$\begin{aligned} \mathbf{q}_{LWRIII} &= (0 \ 90 \ -90 \ 0 \ 0 \ -90 \ 147)^\circ \\ \mathbf{q}_{KR3} &= (-45 \ -25 \ -10 \ 90 \ 90 \ -50)^\circ \\ \mathbf{q}_{KR6} &= (16 \ 5 \ 58 \ 89 \ 90 \ 54)^\circ \\ \mathbf{q}_{KR500} &= (11 \ -7 \ 55 \ 30 \ -19 \ -25)^\circ. \end{aligned}$$

The reflected Cartesian inertia in impact direction for the evaluated configurations is given in Tab. I along with a very short comparison on the robot key facts. A feature of the KR3-SI (a “safe” robot designed for human-robot interaction) which has to be mentioned is the safeguarding of the tool by means of an intermediate flange with breakaway function. This triggers the emergency stop in case the contact force at the TCP exceeds a certain threshold<sup>4</sup>. In combination with the mounted impactor its weight is 1.4 kg.

Robot	Weight [kg]	Nom. Load [kg]	Ref. Inertia [kg]
LWRIII	14	14	4
Kuka KR3-SI	54	3	12
Kuka KR6	235	6	67
Kuka KR500	2350	500	1870

TABLE I  
INERTIAL KEY FACTS OF EVALUATED ROBOTS.

### III. RESULTS FOR THE HEAD

#### A. Head Injury Criterion

In Fig. 7 the resulting HIC values for the different robots are visualized for  $\|\dot{x}_R\| \in \{0.7 \ 1.0 \ 1.5 \ 2.0\}$  m/s and additionally classified with respect to the EuroNCAP. The

<sup>3</sup>KUKA KR3-SI, KUKA KR6, and KUKA KR500

<sup>4</sup>Category 0 stop according to DIN EN 60204. This means that the drives are immediately switched off and the brakes engage at the same time.

values for the KR3-SI are even lower than those for the LWRIII because the intermediate flange decouples the impactor during the moment of impact from the entire robot. Therefore, only the flange-impactor complex is involved in the impact. Clearly, the saturation effect explained in Sec. I was observed, as the numerical values for the KR6 or KR500 do not significantly differ. Thus, the simulation results presented in Fig. 1 should be considered as conservative. The actual saturation value is even noticeably lower than predicted. The results indicate a **very low** potential injury occurring during such impacts with respect to the HIC and rated according to the EuroNCAP [13]. The probability of a resulting injury level of AIS  $\geq 3$  obtained by the extended Prasad/Mertz curves<sup>5</sup> is for all robots maximally  $\approx 0.15\%$ , i.e. negligible. The HIC for the KR500 measured at 80 % and 100 % maximum joint velocity  $\dot{q}_1^{\max}$ , corresponding to a Cartesian velocity of 2.9 m/s and 3.7 m/s, was 135 and 246. This means that even such an enormous robot as the KR500 cannot pose a significant threat by means of impact to the human head measured by typical Severity Indices from automobile crash-testing. The injury levels for these values are located in the *green* area and the probabilities of AIS  $\geq 3$ -injuries are 1.2 % and 3.6 % for the faster impacts with the KR500, see Fig. 7.

### B. Head Impact Forces

As shown in Sec. III-A the HIC values for all robots, even for the KR500 at maximum joint velocity in outstretched configuration, are classified as far lower than **low** by means of EuroNCAP<sup>6</sup>. Therefore, other injury mechanisms possibly occurring during human-robot collisions like fractures of cranial & facial bones have to be investigated. This particular injury is motivated by recorded contact forces during impacts which were in the order of the fracture tolerance of these bones, see Tab. II. Contact forces were analyzed during the robot-HIII/dummy-dummy impacts for all four robots and show an interesting behavior, see Fig. 8a-d. Generally, one can see the decreasing impact duration with growing robot speed for all robots. Furthermore, contact forces increase faster with impact velocity, the heavier the robot is. However, at the same time a saturation effect similar to the one of HIC can be observed. The maximum impact force at 2 m/s for the KR6 and KR500 exceeds the force produced by the LWRIII only by 0.5 kN. According to [15] the HIII head has similar impact characteristics to the human frontal area<sup>7</sup> which gives the opportunity to use our real impact measurements to analyze the possibility of fractures of the frontal bones, see Fig. 9.

1) *Fracture Forces:* In Tab. II limits of the facial and cranial bones according to [17], [18] are listed. The corresponding terminology of the head anatomy is illustrated in Fig. 9. Generally, the fracture force highly depends on the contact area used for such tests. Fractures are categorized into linear (well distributed), depressed ( $< 13 \text{ cm}^2$ ) and

<sup>5</sup>For a detailed evaluation please refer to [4].

<sup>6</sup>With cadaver impacts it is shown as well that the head would not be ripped of the body during a very fast impact at 20km/h [14]. However, the actual injury of the neck during such a collision is still under investigation.

<sup>7</sup>However, this is the only area of a HIII head having similar contact properties as the human. Other areas show considerably higher stiffness than its human equivalents and thus cannot be used as a comparison basis.

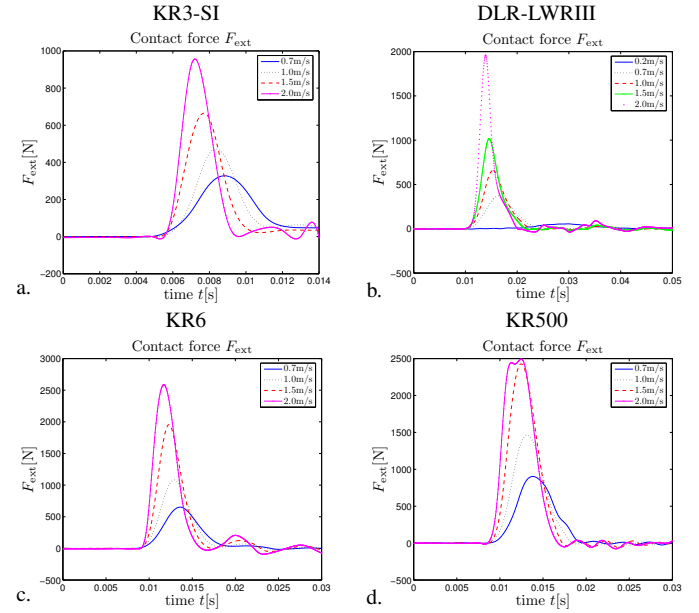


Fig. 8. Measured contact/impact forces of the KUKA KR3-SI, LWRIII, KUKA KR6 and KUKA KR500 colliding with the dummy-dummy at various impact velocities.

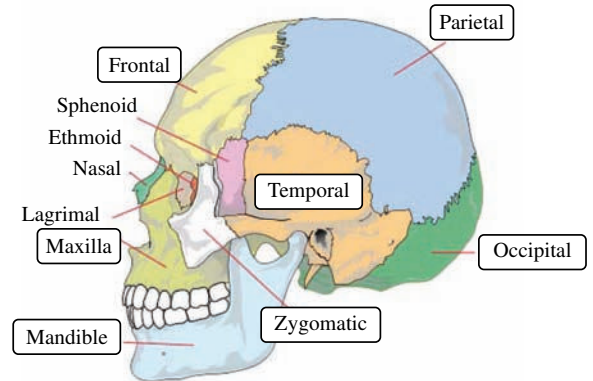


Fig. 9. (Simplified) anatomy of the human skull [16].

Facial bone	FRACTURE FORCE
Mandible (A-P)	1.78 kN
Mandible (lateral)	0.89 kN
Maxilla	0.66 kN
Zygoma	0.89 kN
Cranial bone	FRACTURE FORCE
Frontal	4.0 kN
Temporo-Parietal	3.12 kN
Occipital	6.41 kN

TABLE II  
FACIAL IMPACT TOLERANCE OF CADAVER HEADS.



depressed with punch through fractures ( $< 5 \text{ cm}^2$ ). Linear or simple fracture of the skull is rated with AIS = 2. Comminuted, depressed fracture of  $\leq 2 \text{ cm}$  is rated with AIS = 3. Complex, exposed or loss of brain tissue fracture corresponds to AIS = 4 [19].

2) *Evaluating Real Impact Forces for the Head:* As shown in Tab. II the fracture force of the frontal bone is 4 kN, i.e. it is almost twice as high as the maximum measured forces of 2.5 kN (at velocities up to 2 m/s). As mentioned above, only the frontal bone can be evaluated by HIII (or dummy-dummy) impact tests and since the measured impact forces do not reach critical values for the frontal bone, we carried out impact simulations to judge whether other cranial or facial bones are at risk.

3) *Head Model:* In order to carry out impact simulations, suitable models of the area (bone) of interest are needed: Depending on the contact area we will utilize models obtained by human cadaver tests carried out in [20], [21], [15], [22]. They mainly differ in terms of stiffness and their particular fracture force, see Tab. II.

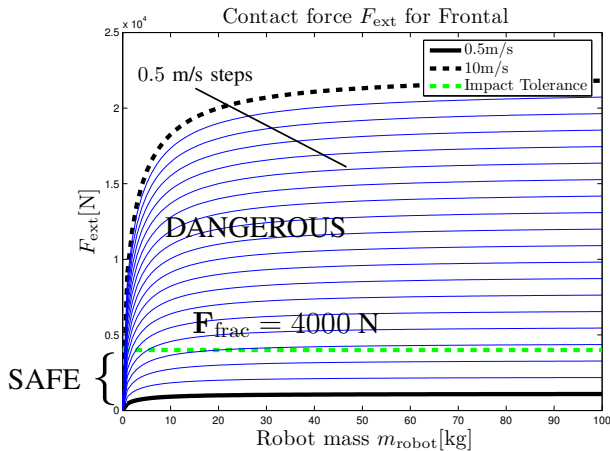


Fig. 10. Contact forces for simulated impacts between a robot and the frontal area showing the dependency on the robot mass and velocity. The impact velocity steps are 0.5 m/s. The stiffness of the frontal bone is  $\approx 10^6 \frac{\text{N}}{\text{m}}$ . Compared to the HIII/dummy-dummy this simulation is conservative.

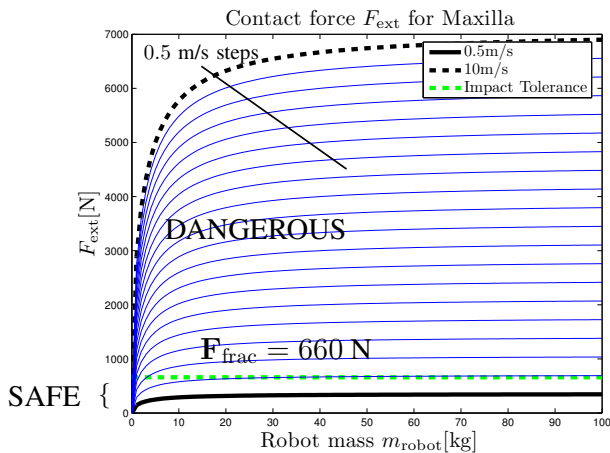


Fig. 11. Contact forces for simulated impacts between a robot and the maxilla showing the dependency on the robot mass and velocity. The impact velocity steps are 0.5 m/s. The stiffness of the maxilla is  $\approx 10^5 \frac{\text{N}}{\text{m}}$ .

4) *Facial Impact simulation:* In Fig. 10, 11 the dependency of the impact force with respect to the robot mass and velocity (the robot is assumed to move with constant velocity) for the frontal bone and the maxilla are visualized. Since the goal of this work is to establish safety limits which ensure the prevention of fractures, the simulations were carried out for worst-case conditions<sup>8</sup>. For all bones<sup>9</sup>, except the frontal one it seems that starting from the saturation mass value<sup>10</sup>, a velocity between 0.5–1.0 m/s is enough to cause fractures. The frontal bone on the other hand is a very resistant one, generally withstanding impacts approximately up to 2 m/s. Furthermore, it becomes clear that especially for robots with less than 5 kg reflected inertia at the moment of impact the velocity can be significantly higher without exceeding the limit contact force. For weaker bones like the maxilla impact speeds of 2 m/s are already posing a major fracture source even for low-inertia robots.

The experiments described in the following validate our assumption of a conservative but nevertheless realistic upper bound. According to [23] following correlation between kinetic impact energy and injury severity by means of frontal fractures for cadaver head drop tests were observed:

- 50–100 J: Drop from 1 – 2 m height (4.6–9.6 m/s). Resulting in simple linear fracture of AIS = 2 or a more severe one of AIS = 3
- 100–200 J: Complicated fracture AIS  $\geq 3$
- $\approx 200 \text{ J}$ : Vascular injury, therefore hematoma. Combination of AIS for skull and brain AIS  $> 3$

Below 50 J usually no fractures occur. An impact velocity of 2 m/s would mean a kinetic energy of 10 J at a drop height of 0.2 m. The impact force would be 4.4 kN for the assumed stiffness of the frontal bone in Fig. 10, implying a fracture already at 10 J. This can be explained by the very conservative estimation of the frontal stiffness which completely neglects the comparatively slowly increasing force in the beginning of an impact [15], [22]. Therefore, Fig. 10 and Fig. 11 are overestimating the resulting injury. However, e.g. in [17] it is shown that frontal fracture can already occur at 2–3 kN for smaller contact areas and [24] indicates frontal fractures already at 37 J<sup>11</sup>. Due to the very significant biomechanical variation found in the literature we chose to assume the most conservative contact stiffness, leading to an upper bound which is conservative in the range of factor 2. Compared to the ISO-10218 which is conservative<sup>12</sup> in the range of more than an order of magnitude (for both, the force and velocity), the suggested limits prevent the strong limitation of robot performance demanded by the ISO-10218.

In order to estimate the consequences after a fracture occurs one has to take into consideration that the applied human model is not valid anymore after the fracture. This

<sup>8</sup>The contact stiffness is assumed to be the worst-case found in the literature.

<sup>9</sup>Simulations for other facial and cranial bones were carried out as well. They show similar behavior.

<sup>10</sup>The robot mass from which on a further increase does not result in significantly higher forces.

<sup>11</sup>An impactor was used, i.e. drop tests with a pre-defined impactor mass were carried out.

<sup>12</sup>Notice that the ISO-10218 impose a velocity limit of 0.25 m/s, corresponding to a drop height of 2 mm.

is because the resistance of the human head is dramatically lowered, possibly causing even more severe injury. A precise statement about these consequences is currently not possible but the experiments according to [23] give first hints. Furthermore, empirical data on cadaver experiments at  $\approx 22$  km/h ( $\approx 6$  m/s) with an impactor of 23 kg exists [14], [25]. Such impacts lead to maximum AIS = 3 injuries for facial impacts, while evaluating the skull, brain, neck, and skin. Important to notice is that the authors state that in reality AIS = 4 is not excluded. Based on these experiments we may presume that, due to the generally highly increasing injury severity with impact velocity, much less severe injury occurs at the typical robot velocities we investigate.

#### IV. RESULTS FOR THE CHEST

##### A. Injury Criteria of the Chest

In this section severity indices for the chest will be introduced. Furthermore, real impact measurements as well as simulations of chest impacts are going to be presented.

1) *Maximum Force*: In [26] impact experiments with volunteers were conducted in order to define a threshold of pain concerning impact force and chest deflection. The maximum **tolerable** contact force was measured to be in the range of

$$F_{\text{ext}}^{x,\text{tol}}(\Delta x_H) \in [1.15 \dots 1.7] \text{ kN}. \quad (2)$$

The obtained values were naturally much smaller than the force limits for injury obtained from cadaver experiments. Henceforth, one should keep in mind that (2) does not indicate physical injury. In order to be able to quantify the actual injury caused by a certain contact force, a linear mapping to the Abbreviated Injury Scale was developed in [27] and is defined as

$$\text{AIS}(F_{\text{ext}}^x(\Delta x_H)) = 0.859 + 0.000652 F_{\text{ext}}^x(\Delta x_H). \quad (3)$$

Important to notice is the minimum value of 0.859, i.e. this least-square fit has to be analyzed with some precaution, especially for smaller contact forces.

2) *Compression-Criterion*: From evaluated cadaver experiments it was derived that acceleration and force criteria alone are intrinsically not able to predict the risk of internal injury of the thorax which tends to be a greater threat to human survival than skeletal injury. Kroell [28], [27] analyzed a large data base of blunt thoracic impact experiments and realized that the Compression Criterion

$$CC = \frac{|\Delta x_H|}{D_c} \leq \Delta_{\text{tol}}, \quad (4)$$

which is the thoracic deflection in [%], is a superior indicator of chest injury severity<sup>13</sup>.  $\Delta x_H$  is the chest deflection and  $D_c$  is the chest A-P diameter<sup>14</sup>. Especially sternal impact was shown to cause compression of the chest until rib fractures occur [30], [31]. The  $CC$  correlates with injury severity via its AIS-level by

$$\text{AIS}(CC) = -3.78 + 19.56CC. \quad (5)$$

<sup>13</sup>In the EuroNCAP the chest deflection is not normalized.

<sup>14</sup>A-P = Anterior-Posterior, assumed to be 221mm [29].

(5) should be used carefully as well because this simple regression is based on impact data at quite high velocities of  $\geq 4$  m/s. In addition to (5), mappings to injury probability with logistic regression models were defined in [32], [33]. Apart from the presented criteria the very prominent Viscous Criterion (VC) exists, which is going to be evaluated here as well and was previously described in [4]. We will investigate various chest criteria to ensure the evaluation of the different injury mechanisms which are covered by them.

##### B. Evaluating Real Impact Forces for the Chest

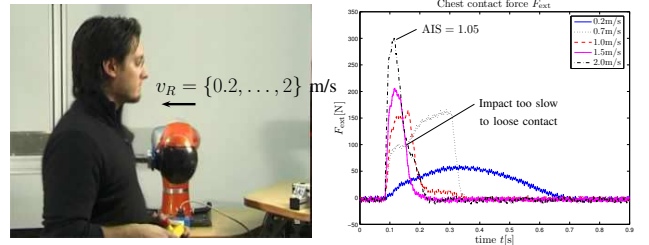


Fig. 12. Contact forces for real impacts between the LWRIII in position control and a volunteer for various impact velocities. If the impact velocity is high enough the contact duration is  $\leq 100$  ms. The robot does not react to the collision, i.e. continues to follow its desired trajectory.

In Fig. 12 the impact forces occurring during real impacts between the LWRIII and a human for the same trajectory as in [4] are given for impact velocities up to 2 m/s. The forces are even at this velocity approximately only one fourth of the tolerable value given in (2). The corresponding maximum AIS value for an impact velocity of 2 m/s is 1.05, i.e. slightly above the offset in (3). This result indicates that no injury potential is caused by impact forces at such speeds for the chest. In order to give a more general statement, impact simulations with robots of increasing mass and velocity were carried out, pointing out under what conditions blunt impacts can become potentially dangerous to the human chest.

##### C. Chest Impact Simulations

1) *Chest Model*: In [34] human chest models for blunt thoracic impacts of human cadavers and HIIIs was presented. This model was developed from impact experiments with human cadaver, volunteers and dummies. For our analysis we use the human cadaver fit<sup>15</sup>.

2) *Simulation Results*: In Fig. 13a-c the resulting severity index and corresponding injury probability are shown as a function of robot mass and parameterized by the impact velocity up to 3 m/s. The injury level (probability) is indicated for the simulated range and for CC and VC the corresponding EuroNCAP injury level is given as well<sup>16</sup>. As for the head a saturation effect is occurring for free impacts for all injury measures. The injury probability of the Compression Criterion fulfills  $p(\text{AIS} \geq 1) \leq 50$  %. The EuroNCAP is a somewhat more restrictive rating and velocities of more than 1.0 m/s can exceed the green indicated area for large robots. This is not the case for the LWRIII, staying even for 3 m/s below 22 mm which also corresponds to Sec. IV-B and [4],

<sup>15</sup>Please note that the human is basically reduced to a torso for this analysis.

<sup>16</sup>Please note that the EuroNCAP is defined for dummies.

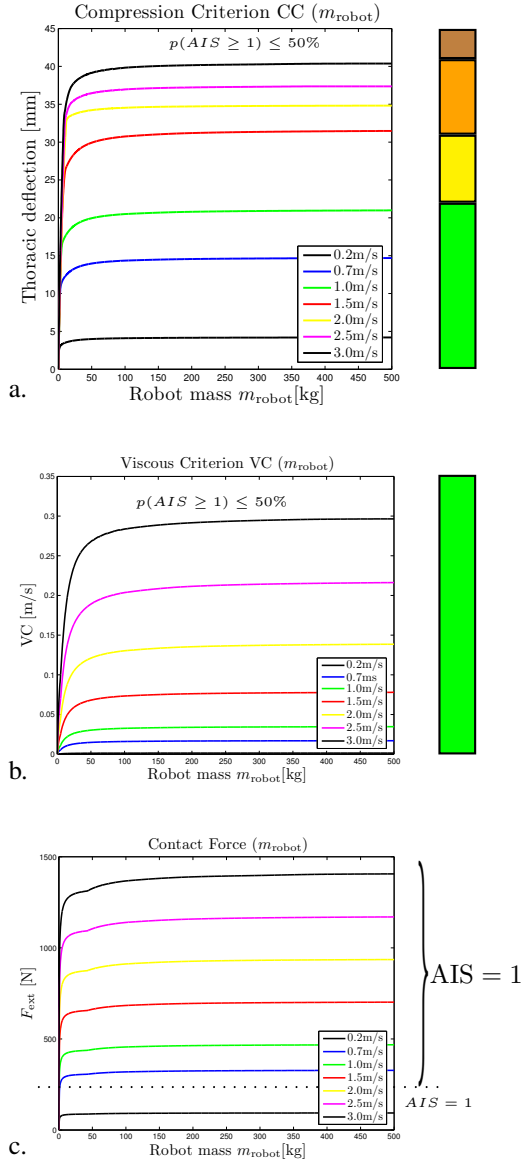


Fig. 13. Resulting CC (a.), VC (b.) and Contact force (c.) values for varying impact robot velocities and masses. Additionally, the correlation to AIS is indicated [33], [35], [27].

[11]. The Viscous Criterion seems not to be an appropriate measure because it is not a very sensitive indicator at the investigated low velocities. This confirms the assumptions already made in [4]. For impacts of arbitrary robot mass and velocities up to 3 m/s both, the EuroNCAP rating and the probability mapping of the VC, developed in [35], indicate very low injury. Similar to CC and VC, the contact force indicates very low injury. The tolerance level (2) cannot be exceeded by increasing robot mass, supported by the fact that the AIS = 2 line is not crossed.

Of course the next issue worth to be evaluated is at which impact velocities dangerous injuries may occur. In Fig. 14 trajectories of the CC, VC and  $F_{ext}$  are plotted for impacts at impact velocities in the range of  $0.5 \leq \|\dot{\mathbf{x}}_R\| \leq 10$  m/s for a 10 kg and a 500 kg robot. Velocities lower than 4.5 m/s are not producing very high injuries in general. In order not to

exceed the maximum tolerable impact force (2) one should not drive faster than  $\approx 5.5$  m/s with the 10 kg robot and  $\approx 3.5$  m/s with the 500 kg robot.

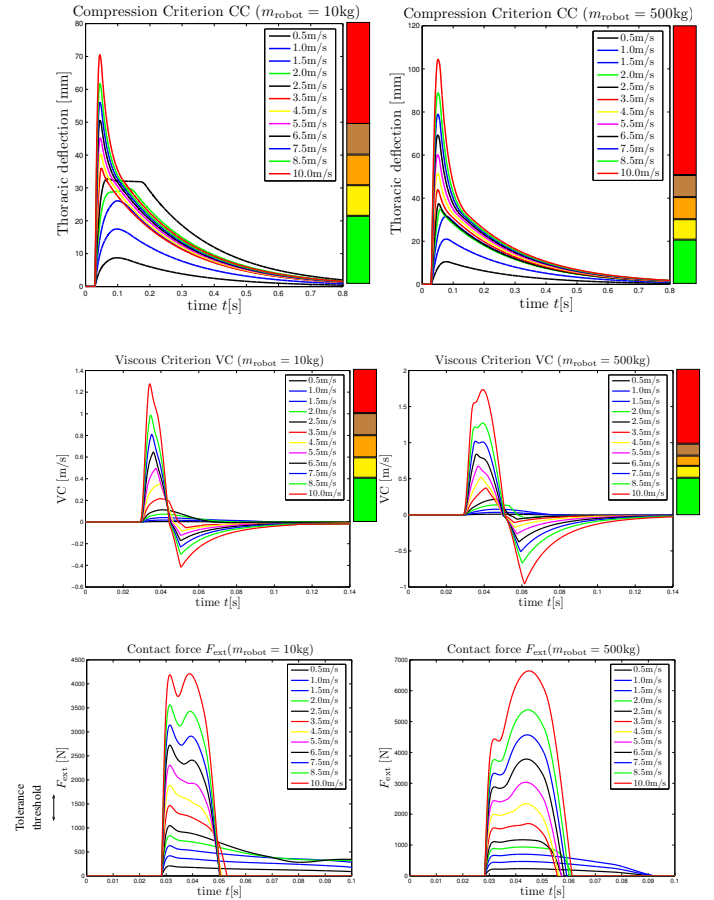


Fig. 14. Severity indices for simulated robot-chest impacts at various impact velocities for a 10 kg (left) and a 500 kg robot (right). For the CC and VC the corresponding EuroNCAP color code is indicated.

#### D. An intuitive Example: The Soccer Kick

In order to show by a very intuitive experiment that a non-constrained impact is very unlikely to be life threatening<sup>17</sup>, a soccer ball was kicked with the KUKA KR500 at maximum joint velocity (see the attached video). The ball hits the ground after a flight of only  $\approx 2$  m. In comparison, a human performed a kick as well, showing how slowly and carefully he hits the ball in order not to shoot farther. Additionally, a rather hard shot was taken to visualize the dramatic contrast to the robot. This example gives a better feeling of what it means to be hit by a real robot.

#### V. CONCLUSION & OUTLOOK

We proved via experiment the statement given in [4] that potential injury of the head indicated by HIC, occurring during an impact, will saturate with increasing robot mass and is from a certain robot mass on only depending on the impact velocity. Typical severity indices focusing just on the moment of impact like the Head Injury Criterion are not an

<sup>17</sup>Except for very pathological cases.

appropriate measure of injury severity in robotics because no robot exceeds their safety critical thresholds. This is due to the usually significantly lower velocities of the robots compared to impact tests carried out in automobile crash-testing. Summarized, blunt head impacts without clamping at moderate robot speed are, no matter how massive the robot is, very unlikely to be life-threatening<sup>18</sup>. This statement was also supported by the soccer ball kick carried out with the KUKA KR500. It shows that the speed of the robot is the major factor defining possible injury severity. However, other less dangerous injuries by means of AIS, as fractures of facial and cranial bones, can occur already at typical high robot velocities and seem to be a more relevant injury mechanism for investigation. Moreover, the question arises what secondary injuries are possible after a fracture (e.g. of a cranial bone) occurred. These cannot be evaluated with the current simulations and need further investigation.

To our knowledge our measurements are the first of this kind carried out for various different robots, ranging from manipulators especially designed for physical human-robot interaction to various types of industrial robots with increasing weight.

Although the type of impact investigated in this paper is unlikely to **severely** injure a human there are other threats still to be investigated. Very different observations can be made in case of clamping which is discussed in the second part of this work [11]. In case of clamping both the head and chest can be severely injured, even leading to death.

A **video** illustrating and supporting some key aspects proposed and explained in the paper is attached and further ones can be found at [www.robotic.dlr.de/safe-robot](http://www.robotic.dlr.de/safe-robot).

#### ACKNOWLEDGMENT

We would like to thank Dr. Peter Heiligensetzer for supporting us with the KUKA KR3-SI impact tests. Furthermore, many thanks to Oliver Eiberger and Mirko Frommberger who were an enormous help at building up the dummy-dummy and conducting the impact tests. Our special gratitude goes to Professor Dimitrios Kallieris for sharing his enormous biomechanical knowledge with us.

#### REFERENCES

- [1] I. Asimov, *The Caves Of Steel, A Robot Novel*, 1954.
- [2] A. Bicchi and G. Tonietti, "Fast and Soft Arm Tactics: Dealing with the Safety-Performance Trade-Off in Robot Arms Design and Control," *IEEE Robotics and Automation Mag.*, vol. 11, pp. 22–33, 2004.
- [3] M. Zinn, O. Khatib, and B. Roth, "A New Actuation Approach for Human Friendly Robot Design," *Int. J. of Robotics Research*, vol. 23, pp. 379–398, 2004.
- [4] S. Haddadin, A. Albu-Schäffer, and G. Hirzinger, "Safety Evaluation of Physical Human-Robot Interaction via Crash-Testing," *Robotics: Science and Systems Conference (RSS2007)*, Atlanta, USA, 2007.
- [5] ISO10218, "Robots for industrial environments - Safety requirements - Part 1: Robot," 2006.
- [6] K. Ikuta, H. Ishii, and M. Nokata, "Safety Evaluation Method of Design and Control for Human-Care Robots," *Int. J. of Robotics Research*, vol. 22, no. 5, pp. 281–298, 2003.
- [7] J. Heinzmann and A. Zelinsky, "Quantitative Safety Guarantees for Physical Human-Robot Interaction," *Int. J. of Robotics Research*, vol. 22, no. 7-8, pp. 479–504, 2003.
- [8] H.-O. Lim and K. Tanie, "Human Safety Mechanisms of Human-Friendly Robots: Passive Viscoelastic Trunk and Passively Movable Base," *Int. J. of Robotics Research*, vol. 19, no. 4, pp. 307–335, 2000.

- [9] S. Haddadin, A. Albu-Schäffer, and G. Hirzinger, "Approaching Asimov's 1st Law," *HRI Caught on Film, ACM/IEEE International Conference on Human-Robot Interaction (HRI2007)*, Washington DC, USA, pp. 177–184.
- [10] J. Versace, "A Review of the Severity Index," *Proc 15th Stapp Conference*, vol. SAE Paper No.710881, 1971.
- [11] S. Haddadin, A. Albu-Schäffer, and G. Hirzinger, "The Role of the Robot Mass and Velocity in Physical Human-Robot Interaction - Part II: Constrained Blunt Impacts," *IEEE Int. Conf. on Robotics and Automation (ICRA 2008)*, Pasadena, USA, 2008.
- [12] —, "Approaching Asimov's 1st Law: The Impact of the Robot's Weight Class," *Robotics: Science and Systems Conference Workshop: Robot Manipulation: Sensing and adapting the real world (RSS2007)*, Atlanta, USA, 2007.
- [13] EuroNCAP, "European Protocol New Assessment Programme - Assessment Protocol and Biomechanical Limits," 2003.
- [14] A. Rizzetti, D. Kallieris, P. Schiemann, and P. Mattern, "Response and Injury of the Head-Neck Unit during a Low Velocity Head Impact," *Int. Conf. on the Biomechanics on Impact (IRCOBI1997)*, Hanover, Germany, pp. 194–207, 1997.
- [15] D. L. Allsop, C. Y. Warner, M. G. Wille, D. C. Schneider, and A. M. Nahum, "Facial Impact Response-A Comparison of the Hybrid III Dummy and Human Cadaver," *SAE Paper No.881719, Proc. 32th Stapp Car Crash Conference*, pp. 781–797, 1988.
- [16] "Wikipedia, the free encyclopedia," <http://en.wikipedia.org>.
- [17] J. Melvin, "Human Tolerance to Impact Conditions as related to Motor Vehicle Design," *SAE J885 APR80*, 1980.
- [18] E. C. Framework, "Improved Frontal Impact Protection through a World Frontal Impact Dummy," *Project No. GRD1 1999-10559*, 2003.
- [19] D. Kallieris, *Handbuch gerichtliche Medizin*, B. Brinkmann and B. Madea, Eds. Springer Verlag, 2004.
- [20] G. W. Nyquist, J. M. Cavanaugh, S. J. Goldberg, and A. I. King, "Facial Impact Tolerance and Response," *SAE Paper No.861896, Proc. 30th Stapp Car Crash Conference*, pp. 733–754, 1986.
- [21] J. McElhaney, R. Stalnaker, and V. Roberts, "Biomechanical Aspects of Head Injury," *Human Impact Response - Measurement and Simulation*, 1972.
- [22] D. L. Allsop and C. Y. Perl, Thomas R. and Warner, "Force/Deflection and Fracture Characteristics of the Temporo-parietal Region of the Human Head," *SAE Transactions*, pp. 2009–2018, 1991.
- [23] D. Kallieris, "Personal communication."
- [24] D. C. Schneider and A. M. Nahum, "Impact Studies of Facial Bones and Skull," *SAE Paper No.720965, Proc. 16th Stapp Car Crash Conference*, pp. 186–204, 1972.
- [25] D. Kallieris, "Schutzkriterien für den menschlichen Kopf," *Forschungsprojekt FP 2.93172*, 1998.
- [26] L. Patrick, "Impact Force Deflection of the Human Thorax," *SAE Paper No.811014, Proc. 25th Stapp Car Crash Conference*, pp. 471–496, 1981.
- [27] C. Kroell, D. Scheider, and A. Nahum, "Impact Tolerance and Response of the Human Thorax II," *SAE Paper No.741187, Proc. 18th Stapp Car Crash Conference*, pp. 383–457, 1974.
- [28] —, "Impact Tolerance and Response of the Human Thorax," *SAE Paper No.710851, Proc. 15th Stapp Car Crash Conference*, pp. 84–134, 1971.
- [29] G. Ryan, D. Hendrie, and N. Mullan, "Development of a Method of Estimating the Costs of Injuries Predicted by ANCAP Testing in Australia," *Proceedings of 1998 Road Safety & Research Enforcement Conference*, pp. 2526–2531, 1998.
- [30] I. Lau and D. Viano, "Role of Impact Velocity and Chest Compression in Thoracic Injury," *Avia. Space Environ. Med.*, vol. 56, 1983.
- [31] —, "The Viscous Criterion - Bases and Applications of an Injury Severity Index for Soft Tissues," *Proceedings of 30th Stapp Car Crash Conference*, vol. SAE Technical Paper No. 861882, 1986.
- [32] R. Eppinger, E. Sun, F. Bandak, M. Haffner, N. Khaewpong, M. Maltese, S. Kuppa, T. Nguyen, E. Takhounts, R. Tannous, A. Zhang, and R. Saul, "Development of Improved Injury Criteria for the Assessment of Advanced Automotive Restraint System - II," *NHTSA Report*, 1999.
- [33] J. A. Newman, S. Tylko, and T. Miller, "Toward A Comprehensive Biomechanical Injury Cost Model," *Accident Analysis and Prevention*, vol. 3, pp. 305–314, 1994.
- [34] T. Lobdell, C. Kroell, D. Scheider, and W. Hering, "Impact Response of the Human Thorax," *Symposium on Human Impact Response*, pp. 201–245, 1972.
- [35] R. Lowne and E. Jansen, "Thorax Injury Probability estimated using Production Prototype EuroSID," *Unpublished working notes from Working Group ISO/TC22/SC12/GT6 N302*.

<sup>18</sup>The presented evaluation is carried out for average males and not for females or children.